NASA TECHNICAL NOTE

NASA TN D-3543

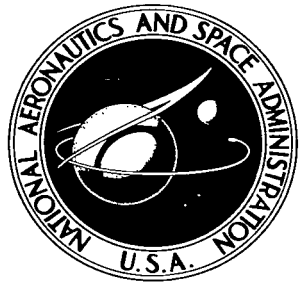

THERMAL DISTORTIONS OF THIN-WALLED PARABOLOIDAL SHELLS

by Joseph E. Walz

Langley Research Center
Langley Station, Hampton, Va.

NATIONAL AERONAUTICS AND SPACE ADMINISTRATION • WASHINGTON, D. C. • AUGUST 1966

NASA TN D-3543

THERMAL DISTORTIONS OF THIN-WALLED PARABOLOIDAL SHELLS

By Joseph E. Walz

Langley Research Center
Langley Station, Hampton, Va.

NATIONAL AERONAUTICS AND SPACE ADMINISTRATION

For sale by the Clearinghouse for Federal Scientific and Technical Information
Springfield, Virginia 22151 – Price $2.00

THERMAL DISTORTIONS OF THIN-WALLED PARABOLOIDAL SHELLS*

By Joseph E. Walz
Langley Research Center

SUMMARY

Equations are presented to describe the linear behavior of a deep thin-walled shell of revolution subjected to an axisymmetric thermal loading. A solution is obtained for a paraboloid with a ring at the edge. Results are plotted showing the rotation of the tangent to the shell due to (1) constant temperature difference between shell and ring and (2) constant temperature gradient through the thickness of the shell.

INTRODUCTION

The radiation of the sun provides an attractive source of power for satellites and space vehicles. To transform the radiation of the sun into electrical power, a conversion system is required. In order to obtain usable amounts of electrical power, some conversion systems require concentration of the rays of the sun; thus, the concept of a solar concentrator has been developed. Several shapes of concentrators are conceivable, but most of the attention has been devoted to the paraboloidal shape because of its high concentrating ability. In the utilization of a paraboloidal mirror as a solar concentrator, the question arises as to the effect that temperature gradients have on the shape of the shell forming this mirror and consequently on its concentrating ability.

In order to obtain maximum efficiency, efforts will be made to train the axis of the paraboloidal mirror directly at the center of the sun; hence, axisymmetric temperature effects may be encountered. In preliminary studies (such as ref. 1) where the use of linear plate formulas have been employed, temperature gradients through the thickness of the paraboloid were shown to produce large overall distortions. Reference 2 develops a means of solving the general axisymmetric thermal problem for an isotropic shell of revolution which is based on deep shell theory; unfortunately, the numerical results in the illustrative example section appear to be in error.

---

*The information presented herein is based in part upon a thesis submitted in partial fulfillment of the requirements for the degree of Master of Science in Engineering Mechanics, Virginia Polytechnic Institute, Blacksburg, Virginia, June 1965.

In the present paper equations governing the linear behavior of a general isotropic shell of revolution subjected to an axisymmetric temperature distribution are given. Deep shell theory, although different from that used in reference 2, is employed to obtain these equations. These equations are specialized for a paraboloid with a ring at the edge subjected to a constant overall temperature change and a constant temperature gradient through the thickness; the ring may have a uniform temperature change which is different from that of the shell. The ability of the ring to restrict the expansion and rotation of the edge of the shell can be varied by adjusting the stiffness parameters involved. Results are presented in equation form for stresses and displacements, and figures showing rotation of the tangent at any location are plotted for a wide range of parameters. An indication is given as to the effect that thermal distortions have on the concentrating ability of a paraboloid used as a solar concentrator.

SYMBOLS

The units used for the physical quantities defined in this paper are given both in U.S. Customary Units and in the International System of Units (SI). (See ref. 3.)

A_r cross-sectional area of ring

a radius from axis to centroid of ring (see fig. 3)

b cross-sectional radius of circular ring (see fig. 3)

C extensional stiffness of shell, Eh

$\overline{C}$ dimensionless ratio of extensional stiffness of ring to that of shell, $\frac{E_r A_r}{Ehr_o}$

C_A concentration ratio herein used as ratio of projected area of concentrator to area of aperture of an absorber located in focal plane

D flexural stiffness of shell, $\frac{Eh^3}{12(1 - \nu^2)}$

$\overline{D}$ dimensionless ratio of flexural stiffness of ring to that of shell, $\frac{E_r I_r}{r_o D}$

E Young's modulus of shell

E_r Young's modulus of ring

e_h radial eccentricity of centroid of ring from point of attachment of ring to shell (see fig. 3)

e_v axial eccentricity of centroid of ring from point of attachment of ring to shell (see fig. 3)

$F(k,\chi)$ elliptic integral of first kind, $\int_0^{\chi} \frac{d\chi}{\sqrt{1 - k^2 \sin^2 \chi}}$

f focal length of paraboloid, $\frac{r_o^2}{4z_o}$

H radial stress resultant

h thickness of shell

I_r moment of inertia of cross section of ring about centroidal axis in plane of ring

$i = \sqrt{-1}$

i,j integers

K_1,K_2 constants

k modulus of elliptic integral

l distance in focal plane that a reflected ray misses focal point

l_a radius of aperture of absorber

M_ξ,M_θ bending moments per unit length of sections of shell (see fig. 1)

m applied uniform moment per unit length

N_ξ,N_θ normal stress resultants in meridional and circumferential directions, respectively (see fig. 1)

P applied uniform force per unit length

p_h radially distributed loading, positive in +r-direction

p_v axially distributed loading, positive in +z-direction

Q transverse shear stress resultant

r radial distance to point on meridian of shell

r_o radial distance to edge of shell

T temperature change from stress-free datum

$\Delta T = T_{inner} - T_{outer}$

T_{inner} temperature change from datum of point on inner surface of shell

T_{outer} temperature change from datum of point on outer surface of shell

T_r uniform temperature change of ring from datum

$T_s = \frac{T_{outer} + T_{inner}}{2}$

u radial displacement of shell

$\bar{u}$ nondimensional radial displacement of shell

u_a total radial displacement of attachment point of ring

u_{ac1}, u_{ac2} radial displacements of point of attachment relative to centroid of ring

u_{c1}, u_{c2} radial displacements of centroid of ring

V axial stress resultant

w axial displacement

$\bar{w}$ nondimensional axial displacement

$$X = \sqrt{\frac{rD}{\bar{\alpha}}}\,\beta$$

$$Y = \sqrt{\frac{r}{C\bar{\alpha}}}\,rH$$

z	axial distance to point on meridian of shell
z_o	axial distance to edge of shell
$\bar{\alpha}$	Lamé parameter defined by equation (13a); specialized for paraboloid by equation (38)
α_r	coefficient of linear thermal expansion of ring material
α_s	coefficient of linear thermal expansion of shell material
β	rotation of tangent of point on middle surface of shell from undeformed position to deformed position (see fig. 1)
γ	rim angle
δ_{ij}	Kronecker delta ($\delta_{ij} = 0$, if $i \neq j$; $\delta_{ij} = 1$, if $i = j$)
$\epsilon_\xi, \epsilon_\theta$	strain in meridional and circumferential directions, respectively, at any point in shell
$\bar{\epsilon}_\xi, \bar{\epsilon}_\theta$	strain in meridional and circumferential directions, respectively, at points on middle surface of shell
ζ	coordinate along inward normal of shell (see fig. 1)
η	expression defined by equation (41); specialized for paraboloid by equation (42)
θ	circumferential coordinate
$\kappa_\xi, \kappa_\theta$	curvature changes in meridional and circumferential directions, respectively

λ parameter indicating amount of concavity of paraboloid, $\left(\frac{r_o}{2f}\right)^2$

ν Poisson's ratio of shell material

ξ dimensionless coordinate specifying point on meridian, $\frac{r}{r_o}$

ρ expression defined in equations (28); specialized for paraboloid by equation (39)

$\sigma_\xi, \sigma_\theta$ normal stress in meridional and circumferential directions, respectively

Φ expression defined in equations (28); specialized for paraboloid by equation (40)

φ angle that tangent to a point on undeformed middle surface of shell makes with plane perpendicular to axis of shell (see fig. 1)

χ amplitude of elliptic integral

Subscript:

o evaluated at $\xi = 1$

Primes denote derivatives with respect to ξ.

LINEAR AXISYMMETRIC SHELL EQUATIONS

The governing equations for a linear thermoelastic axisymmetric problem involving a shell of revolution are obtained by modifying the equations in reference 4 to include temperature effects. The positive directions of the stress resultants and couples, displacements, and rotation involved in the development of these equations are shown in figure 1.

Stress-Strain Relations

When transverse normal stress is neglected, the following stress strain relations hold as long as E, α_s, and ν are taken to be constant over the range of temperatures being considered:

$$(1 - \nu^2)\sigma_\xi = E\left(\epsilon_\xi + \nu\epsilon_\theta\right) - E\alpha_s T(1 + \nu) \tag{1}$$

$$(1 - \nu^2)\sigma_\theta = E\left(\epsilon_\theta + \nu\epsilon_\xi\right) - E\alpha_s T(1 + \nu) \tag{2}$$

The assumption is made that the temperature is linear through the thickness of the shell; thus

$$T = T_s + \frac{\zeta}{h}\Delta T \tag{3}$$

where

$$T_s = \frac{1}{2}\left(T_{inner} + T_{outer}\right) \tag{4}$$

$$\Delta T = T_{inner} - T_{outer} \tag{5}$$

The following strain variations through the thickness are used (ref. 4) when attention is restricted to thin shells (that is, ratio of shell thickness to radius of curvature is small compared with one):

$$\left.\begin{aligned}\epsilon_\xi &= \bar{\epsilon}_\xi + \zeta\kappa_\xi \\ \epsilon_\theta &= \bar{\epsilon}_\theta + \zeta\kappa_\theta\end{aligned}\right\} \tag{6}$$

In obtaining the relationships expressed in equations (6), the deformations due to transverse shear and transverse normal stress are neglected; thus, points on the normal to the undeformed surface lie on the normal to the deformed surface. The stress resultants and couples are defined as

$$\left.\begin{aligned}N_\xi &= \int_{-h/2}^{h/2} \sigma_\xi \, d\zeta \\ N_\theta &= \int_{-h/2}^{h/2} \sigma_\theta \, d\zeta \\ M_\xi &= \int_{-h/2}^{h/2} \sigma_\xi \zeta \, d\zeta \\ M_\theta &= \int_{-h/2}^{h/2} \sigma_\theta \zeta \, d\zeta\end{aligned}\right\} \tag{7}$$

Substitutions from equations (1), (2), (3), and (6) into equations (7), after performing the required integrations, yield

$$\left.\begin{aligned} N_\xi &= \frac{C}{1-\nu^2}\left(\bar{\epsilon}_\xi + \nu\bar{\epsilon}_\theta\right) - \frac{C\alpha_s T_s}{1-\nu} \\ N_\theta &= \frac{C}{1-\nu^2}\left(\bar{\epsilon}_\theta + \nu\bar{\epsilon}_\xi\right) - \frac{C\alpha_s T_s}{1-\nu} \\ M_\xi &= D\left(\kappa_\xi + \nu\kappa_\theta\right) - D(1+\nu)\frac{\alpha_s \Delta T}{h} \\ M_\theta &= D\left(\kappa_\theta + \nu\kappa_\xi\right) - D(1+\nu)\frac{\alpha_s \Delta T}{h} \end{aligned}\right\} \tag{8}$$

where

$$\left.\begin{aligned} C &= Eh \\ D &= \frac{Eh^3}{12(1-\nu^2)} \end{aligned}\right\} \tag{9}$$

Equilibrium and Compatibility Equations

Equilibrium of forces in the axial and radial directions is found in reference 4 to be (H is the radial force resultant; V is the axial force resultant (see fig. 1))

$$(rV)' + r\bar{\alpha}p_v = 0 \tag{10}$$

$$(rH)' - \bar{\alpha}N_\theta + r\bar{\alpha}p_h = 0 \tag{11}$$

and the moment equilibrium equation is

$$\left(rM_\xi\right)' - \bar{\alpha}M_\theta \cos\varphi + r\bar{\alpha}(H \sin\varphi - V \cos\varphi) = 0 \tag{12}$$

where a prime denotes differentiation with respect to ξ, and

$$\bar{\alpha} = \left[(r')^2 + (z')^2\right]^{1/2} \tag{13a}$$

$$\tan\varphi = \frac{z'}{r'} \tag{13b}$$

A compatibility relation is given which for small rotations β is

$$\left(r\bar{\epsilon}_\theta\right)' - r'\bar{\epsilon}_\xi = r'\beta \tan \varphi \tag{14}$$

Strain Displacement Relations

Strain displacement equations given in reference 4 are

$$\bar{\epsilon}_\theta = \frac{u}{r} \tag{15}$$

and for small rotations

$$\bar{\epsilon}_\xi = \frac{w' + r'\beta}{z'} \tag{16}$$

where u and w are radial and axial displacements, respectively. Thus, substitution of strains from equations (8) into equations (15) and (16) yields

$$u = \frac{r}{C}\left(N_\theta - \nu N_\xi\right) + r\alpha_S T_S \tag{17}$$

$$w = \int \left[\frac{z'}{C}\left(N_\xi - \nu N_\theta\right) - r'\beta\right]d\xi + \int z'\alpha_S T_S \, d\xi \tag{18}$$

The curvature changes are given as

$$\kappa_\xi = \frac{\beta'}{\bar{\alpha}} \tag{19}$$

and for small rotation

$$\kappa_\theta = \frac{\beta \cos \varphi}{r} \tag{20}$$

Development of Governing Second-Order Differential Equations

The complete system of field equations can be reduced to two ordinary second-order differential equations in two unknowns. To develop these equations, it is desirable, initially, to express all quantities in terms of H, V, β, and the distributed and thermal loads. The normal stress resultant N_ξ and the transverse shear stress resultant Q are related to the axial and radial stress resultants by the following equations:

$$N_\xi = H \cos \varphi + V \sin \varphi \tag{21}$$

$$Q = -H \sin \varphi + V \cos \varphi \tag{22}$$

Once p_V is established, the solution for V from equation (10) is

$$V = -\frac{1}{r} \int r \bar{\alpha} p_V \, d\xi \tag{23}$$

Substitution of the moment expressions in equations (8) into the moment equilibrium equation (12) after first using the curvature changes given in equations (19) and (20) yields a second-order differential equation involving β and rH. The other differential equation required is obtained by substitution of $\bar{\epsilon}_\theta$ and $\bar{\epsilon}_\xi$ from equations (8), with N_θ and N_ξ from equations (11) and (21), into the compatibility equation (14). By use of the following transformation,

$$X = \sqrt{\frac{rD}{\bar{\alpha}}} \, \beta \tag{24}$$

$$Y = \sqrt{\frac{r}{C\bar{\alpha}}} (rH) \tag{25}$$

the two differential equations so derived become

$$X'' - \Theta X + 2\left(\frac{z'}{|z'|}\right)\rho^2 \Phi^2 Y = G_1 + (1 + \nu)\left(\frac{\bar{\alpha} r}{D}\right)^{1/2}\left(\frac{D \alpha_S \Delta T}{h}\right)' \tag{26}$$

$$Y'' - \psi Y - 2\left(\frac{z'}{|z'|}\right)\rho^2 \Phi^2 X = G_2 - (r\bar{\alpha}C)^{1/2}\left(\alpha_S T_S\right)' \tag{27}$$

where

$$\left.\begin{aligned} \rho^2 &= \sqrt{3(1 - \nu^2)}\left|\frac{z'\bar{\alpha}}{rh}\right|_{ref} \\ \Phi^2 &= \frac{\left|\frac{z'\bar{\alpha}}{rh}\right|}{\left|\frac{z'\bar{\alpha}}{rh}\right|_{ref}} \end{aligned}\right\} \tag{28}$$

Equation continued on next page

$$
\left.
\begin{aligned}
\Theta &= \left(\frac{r'}{r}\right)^2 - \frac{\nu\left(\frac{r'D}{\bar{\alpha}}\right)'}{\left(\frac{rD}{\bar{\alpha}}\right)} + \frac{1}{2}\left[\frac{\left(\frac{rD}{\bar{\alpha}}\right)'}{\left(\frac{rD}{\bar{\alpha}}\right)}\right]' + \frac{1}{4}\left[\frac{\left(\frac{rD}{\bar{\alpha}}\right)'}{\left(\frac{rD}{\bar{\alpha}}\right)}\right]^2 \\
\psi &= \left(\frac{r'}{r}\right)^2 + \frac{\nu\left(\frac{r'}{C\bar{\alpha}}\right)'}{\left(\frac{r}{C\bar{\alpha}}\right)} + \frac{1}{2}\left[\frac{\left(\frac{r}{C\bar{\alpha}}\right)'}{\left(\frac{r}{C\bar{\alpha}}\right)}\right]' + \frac{1}{4}\left[\frac{\left(\frac{r}{C\bar{\alpha}}\right)'}{\left(\frac{r}{C\bar{\alpha}}\right)}\right]^2 \\
G_1 &= \frac{r'(rV)}{\left(\frac{rD}{\bar{\alpha}}\right)^{1/2}} \\
G_2 &= \left(\frac{r}{C\bar{\alpha}}\right)^{1/2}\left\{\left[\frac{\left(\frac{r}{C\bar{\alpha}}\right)'}{\left(\frac{r}{C\bar{\alpha}}\right)} + \nu\left(\frac{r'}{r}\right)\right]\left(r\bar{\alpha}p_h\right) + \left(r\bar{\alpha}p_h\right)'\right\} \\
&\quad + \left(\frac{r}{C\bar{\alpha}}\right)^{1/2}\left\{\left[\frac{z'\,r'}{r^2} + \frac{\nu\left(\frac{z'}{C\bar{\alpha}}\right)}{\left(\frac{r}{C\bar{\alpha}}\right)}\right](rV) + \nu\left(\frac{z'}{r}\right)(rV)'\right\}
\end{aligned}
\right\} \qquad (28)
$$

and $|\ |_{ref}$ means the absolute value of a quantity evaluated at a suitably chosen reference point on the shell.

Approximate Solution to Governing Equations

It is convenient to consider separately the homogeneous and particular solutions of the equations. In equations (26) and (27) the quantity ρ^2 is, in general, of the order of the ratio of a radius of curvature to the thickness of the shell and is large compared with unity. The functions Θ and ψ appearing in these equations are, in general, of the order of unity provided the shell is such that the thickness is slowly varying (it may not vary appreciably over a distance on the order of $\sqrt{Rh}$, where h is the average thickness

and R is a representative radius of curvature) and provided the functions are not evaluated in a shallow region of the shell. Under these circumstances, for an approximate solution to the homogeneous parts of equations (26) and (27), it would be permissible to omit the Θ and the ψ terms and put the equations in the following form:

$$\left(X_H + iY_H\right)'' - 2i \frac{z'}{|z'|} \rho^2 \Phi^2 \left(X_H + iY_H\right) = 0 \tag{29}$$

where the subscript H refers to the homogeneous part. Reference 4 seeks to obtain an asymptotic solution to equation (29) by considering the following series:

$$X_H = e^{\rho\mu(\xi)}\left(X_1 + X_2\rho^{-1} + X_3\rho^{-2} + \ldots\right) \tag{30}$$

$$Y_H = e^{\rho\mu(\xi)}\left(Y_1 + Y_2\rho^{-1} + Y_3\rho^{-2} + \ldots\right) \tag{31}$$

As in reference 4 the solution of equation (29), except for small terms of order $1/\rho$, is obtained by retaining only the leading terms in the series in equations (30) and (31) to yield

$$X_H + iY_H = \Phi^{-1/2}\left[C_1 e^{(1+i)\rho\int \Phi\, d\xi} + C_2 e^{-(1+i)\rho\int \Phi\, d\xi}\right] \tag{32}$$

where C_1 and C_2 are complex constants, $\frac{z'}{|z'|}$ is taken to be 1, and μ is $\pm(1 + i)\int \Phi\, d\xi$. The case where $\frac{z'}{|z'|} = -1$ requires changing i to -i in the exponents in equation (32).

In the treatment of approximate particular solutions, it is to be observed that the right-hand sides of equations (26) and (27) consist of applied pressure loading terms and thermal loading terms. With the stipulation that the derivative of the pressure loading with respect to ξ is not of order of magnitude greater than the loading itself, conventional membrane theory has been shown to provide an adequate approximate particular solution consistent with retaining only the leading terms in the homogeneous solution (ref. 5). To obtain a particular solution (denoted by subscript P) for the thermal loading under a similar condition, the first two terms on the left-hand sides of equations (27) and (26) would be neglected, and, as a result,

$$X_P = \frac{1}{2\rho^2\Phi^2}\left[(r\bar{\alpha}C)^{1/2}\left(\alpha_s T_s\right)'\right] \tag{33}$$

$$Y_P = \frac{1}{2\rho^2\Phi^2}\left[(1+\nu)\left(\frac{\bar{\alpha}r}{D}\right)^{1/2}\left(\frac{D\alpha_S\,\Delta T}{h}\right)'\right] \tag{34}$$

which correspond to those obtained in reference 6 for constant thickness. As far as stresses are concerned, the retention of these particular solutions appears to be inconsistent with retaining only the leading terms in the homogeneous solution and stresses obtained in this manner are in question; however, meaningful values for the rotation of the tangent may be obtained away from the edge of the shell.

Separation of equation (32) into real and imaginary parts and the addition of the particular solutions yields the complete solution for X and Y. Thus, the deformations may be evaluated once the geometry is specified.

PARABOLOIDAL SHELL WITH EDGE RING

The general equations developed in the preceding sections are now specialized to a paraboloid of revolution of constant thickness with a ring at the edge. In particular, there is no loading other than a thermal loading due to temperature changes, T_S of the shell and T_r of the ring, and constant temperature gradient through the thickness of the shell ΔT. The presence of a ring is considered because a paraboloid used as a solar concentrator may have a support ring attached at its edge, but other boundary conditions such as a free or clamped edge may be realized by suitably adjusting two stiffness parameters of the ring.

The dimensionless coordinate ξ is used to specify a point on the meridian where

$$\xi = \frac{r}{r_o} \tag{35}$$

and r is the radial distance from the axis to the particular point on the meridian and r_o is the radial distance to the edge. In this coordinate system a paraboloid is specified by

$$z = \frac{r^2}{4f} = \frac{1}{2}\lambda^{1/2} r_o \xi^2 \tag{36}$$

where z is the axial location of a point, f is the focal length of the paraboloid, and $\lambda = \left(\frac{r_o}{2f}\right)^2$. The rim angle γ and λ have the relationship expressed by the following equation, and a plot of this relationship is shown in figure 2:

$$\tan \gamma = \frac{2\lambda^{1/2}}{1 - \lambda} \tag{37}$$

The rim angle γ is the angle formed between the axis of the paraboloid and a line passing through a point on the rim and the focus (fig. 2).

The Lamé parameter, given by equation (13a), for a paraboloid in this coordinate system becomes

$$\bar{\alpha} = r_o\sqrt{1 + \lambda\xi^2} \tag{38}$$

and the first two quantities of equations (28) become

$$\rho = \sqrt[4]{3\left(1 - \nu^2\right)}\lambda\sqrt{\frac{r_o}{h}} \tag{39}$$

$$\Phi = \left(1 + \lambda\xi^2\right)^{1/4} \tag{40}$$

when the apex is selected as the reference point. Another quantity η defined as

$$\eta = \rho\int_0^{\xi} \Phi \, d\xi \tag{41}$$

in this coordinate system, becomes

$$\eta = \rho\left[\frac{2}{3}\,\xi\left(1 + \lambda\xi^2\right)^{1/4} + \frac{\sqrt{2}}{3\sqrt{\lambda}}\,F\left(\frac{1}{\sqrt{2}}, \chi\right)\right] \tag{42}$$

where $F(k,\chi) = \int_0^{\chi} \frac{d\chi}{\sqrt{1 - (k)^2\sin^2\chi}}$ is an elliptic integral of the first kind and

$$\chi = \sin^{-1}\left\{\sqrt{2}\,\sin\left[\frac{1}{2}\tan^{-1}\left(\sqrt{\lambda}\xi\right)\right]\right\} \tag{43}$$

The particular solutions X_P and Y_P, as given by equations (33) and (34) are both zero, since no applied loading is considered besides thermal loading, the shell is of constant thickness, and the temperature components are constant. Thus, the homogeneous

solutions of equations (26) and (27) are the complete solutions. For the case of a paraboloid which is closed at the apex, C_2 is equal to zero (ref. 7) and the following solution is obtained:

$$X = \sqrt{Eh^3}\Phi^{-1/2}e^{-(\eta_o-\eta)}\left(K_1 \cos \eta - K_2 \sin \eta\right) \tag{44}$$

$$Y = \sqrt{Eh^3}\Phi^{-1/2}e^{-(\eta_o-\eta)}\left(K_1 \sin \eta + K_2 \cos \eta\right) \tag{45}$$

where K_1 and K_2 are dimensionless constants obtained by nondimensionalizing the real and imaginary parts of C_1. Henceforth, as in equations (44) and (45), the subscript o indicates a quantity evaluated at the point $\xi = 1$. Equations (44) and (45), with the use of equations (24) and (25), permit the evaluation of stresses and deformations once the constants K_1 and K_2 have been evaluated from the boundary conditions.

Deflection and Rotation of Edge of Shell

Boundary conditions for a shell having a ring attached at its edge are such that deformation and force compatibility must be maintained at the attachment point of the ring and the shell. Thus the radial displacement u of the shell at the edge must be equal to the radial displacement of the ring at the point of attachment. Also, if the method of attachment permits transfer of moment, the edge of the shell and the ring must rotate the same amount about an axis perpendicular to the cross section of the ring.

For the shell, from equations (24) and (44), the rotation at any point is

$$\beta = 2\sqrt{3(1 - \nu^2)}\left(1 + \lambda\xi^2\right)^{1/8}\xi^{-1/2}e^{-(\eta_o-\eta)}\left(K_1 \cos \eta - K_2 \sin \eta\right) \tag{46}$$

and thus at the edge of the shell

$$\beta_o = 2\sqrt{3\left(1 - \nu^2\right)}(1 + \lambda)^{1/8}\left(K_1 \cos \eta_o - K_2 \sin \eta_o\right) \tag{47}$$

where the subscript o denotes evaluation at $\xi = 1$. An approximate relation for the u-displacement, based on the consideration that the solution of the governing equations neglects terms of order $1/\rho$ compared with 1, is found from equations (17), (11), (25), and (45) to be

$$u = h\rho\left(1 + \lambda\xi^2\right)^{-1/8}\xi^{1/2}e^{-(\eta_o-\eta)}\left[K_1(\sin \eta + \cos \eta) + K_2(\cos \eta - \sin \eta)\right] + r_o\xi\alpha_s T_s \tag{48}$$

A nondimensionalized radial displacement $\bar{u}$ is obtained by dividing equation (48) by h; thus, at the edge of the shell

$$\bar{u}_o = (1 + \lambda)^{-1/8}\rho\left[K_1\left(\sin \eta_o + \cos \eta_o\right) + K_2\left(\cos \eta_o - \sin \eta_o\right)\right] + \frac{r_o}{h}\alpha_s T_s \tag{49}$$

Deflection and Rotation of Ring

For a ring subjected to a uniform radial loading per unit length P acting in the plane of the ring, there is no rotation; and the displacement u_{c1} in the direction of loading is given by

$$u_{c1} = \frac{Pa^2}{E_r A_r} \tag{50}$$

(See ref. 8.) For a ring subjected to a uniform moment per circumferential length m tending to twist the ring inside out, there is no displacement but a rotation in the direction of the moment such that

$$\beta_r = \frac{ma^2}{E_r I_r} \tag{51}$$

(See ref. 8.) If the ring has attained a uniform temperature increase T_r from initial equilibrium temperature, the centroid of the cross section of the ring has an additional displacement

$$u_{c2} = a\alpha_r T_r \tag{52}$$

Since, in general, the ring is attached at some point other than its centroid, additional effects must be considered. Because the radial force does not act necessarily through the centroid, the moment created by this eccentricity must be included in equation (51). Rotation of the ring produces a relative displacement between the centroid and the point of attachment. For small positive angular rotation β_r, the radial displacement of the point of attachment relative to the centroid is

$$u_{ac1} = e_v\beta_r \tag{53}$$

where e_v is positive when the point of attachment is above the centroid as shown in figure 3. The displacement of the point of attachment relative to the centroid due to T_r is

$$u_{ac2} = -e_h \alpha_r T_r \tag{54}$$

where e_h is positive when the centroid of the ring is at a distance greater than r_o from the axis of the paraboloid. Thus, the total radial displacement u_a of the point of attachment is given by

$$u_a = u_{c1} + u_{c2} + u_{ac1} + u_{ac2} \tag{55}$$

Evaluation of Constants

In the process of evaluating the constants K_1 and K_2 there are three independent temperature terms to consider. It is possible, because of the linearity of the problem, to consider each effect separately and then combine these effects to obtain the total effect. Thus,

$$K_1 = K_{11}\left(\alpha_s T_s\right) + K_{12}\left(\alpha_s \Delta T\right) + K_{13}\left(\alpha_r T_r\right) \tag{56}$$

$$K_2 = K_{21}\left(\alpha_s T_s\right) + K_{22}\left(\alpha_s \Delta T\right) + K_{23}\left(\alpha_r T_r\right) \tag{57}$$

To insure compatibility of the shell-ring structure, the nondimensional radial displacement of the edge of the shell determined from equation (49) is set equal to the nondimensional radial displacement of the point of attachment of the ring determined from the proper nondimensionalization of equation (55). Similarly, the rotation at the edge of the shell determined from equation (47) is set equal to the rotation of the ring determined from equation (51). From force compatibility considerations, the quantities P and m appearing in equations (50) and (51) are

$$Pa = -H_o r_o \tag{58}$$

$$ma = -\left(M_{\xi_o} + H_o e_v\right) r_o \tag{59}$$

(See fig. 3.) After the appropriate quantities from equations (8), (19), (25), (45), (46), (50), (52), (53), (54), (58), and (59) have been substituted into equations (55) and (51), the two aforementioned equalities result in two simultaneous equations which have the form

$$g_{11} K_{1j} + g_{12} K_{2j} = \bar{g}_{1j} \tag{60}$$

$$g_{21}K_{1j} + g_{22}K_{2j} = \bar{g}_{2j} \tag{61}$$

where the subscript j takes on the value 1, 2, or 3, depending on the temperature component of interest and

$$\left.\begin{aligned}
g_{11} &= -\left(\frac{r_o + e_h}{r_o}\right)\sin\eta_o + \bar{C}\,\frac{e_v}{r_o}\,\frac{r_o}{h}\,2\sqrt{3\left(1-\nu^2\right)}\cos\eta_o - \rho\bar{C}(1+\lambda)^{-1/4}\left(\sin\eta_o + \cos\eta_o\right)\\
g_{12} &= -\left(\frac{r_o + e_h}{r_o}\right)\cos\eta_o - \bar{C}\,\frac{e_v}{r_o}\,\frac{r_o}{h}\,2\sqrt{3\left(1-\nu^2\right)}\sin\eta_o - \rho\bar{C}(1+\lambda)^{-1/4}\left(\cos\eta_o - \sin\eta_o\right)\\
g_{21} &= \rho\left(\sin\eta_o - \cos\eta_o\right)(1+\lambda)^{-1/4} - \frac{e_v}{r_o}\,\frac{r_o}{h}\,2\sqrt{3\left(1-\nu^2\right)}\sin\eta_o - \bar{D}\left(\frac{r_o}{r_o + e_h}\right)\cos\eta_o\\
g_{22} &= \rho\left(\sin\eta_o + \cos\eta_o\right)(1+\lambda)^{-1/4} - \frac{e_v}{r_o}\,\frac{r_o}{h}\,2\sqrt{3\left(1-\nu^2\right)}\cos\eta_o + \bar{D}\left(\frac{r_o}{r_o + e_h}\right)\sin\eta_o\\
\bar{g}_{11} &= \bar{C}(1+\lambda)^{-1/8}\,\frac{r_o}{h}\,\alpha_s T_s\\
\bar{g}_{12} &= 0\\
\bar{g}_{13} &= -\bar{C}(1+\lambda)^{-1/8}\,\frac{r_o}{h}\,\alpha_r T_r\\
\bar{g}_{21} &= 0\\
\bar{g}_{22} &= -\frac{r_o}{h}(1+\nu)\,\frac{(1+\lambda)^{-1/8}}{2\sqrt{3\left(1-\nu^2\right)}}\,\alpha_s\,\Delta T\\
\bar{g}_{23} &= 0
\end{aligned}\right\} \tag{62}$$

where

$$\left.\begin{aligned}
\bar{C} &= \frac{E_r A_r}{E h r_o}\\
\bar{D} &= \frac{E_r I_r}{r_o D}
\end{aligned}\right\} \tag{63}$$

Within the limits of the accuracy of the development and solution of equations (26) and (27), the deflections, stress resultants, and couples become approximately

$$\frac{N_{\xi j}}{Eh} = \left(\frac{r_o}{h}\right)^{-1}\left(1 + \lambda\xi^2\right)^{-3/8}\xi^{-3/2}e^{-(\eta_o-\eta)}\left(K_{ij}\sin\eta + K_{2j}\cos\eta\right) \tag{64}$$

$$\frac{Q_j}{Eh} = -\left(\frac{r_o}{h}\right)^{-1}\left(1 + \lambda\xi^2\right)^{-3/8}\lambda^{1/2}\xi^{-1/2}e^{-(\eta_o-\eta)}\left(K_{1j}\sin\eta + K_{2j}\cos\eta\right) \tag{65}$$

$$\frac{N_{\theta j}}{Eh} = \left(\frac{r_o}{h}\right)^{-1/2}\left(1 + \lambda\xi^2\right)^{-1/8}\lambda^{1/4}\sqrt[4]{3\left(1 - \nu^2\right)}\,\xi^{-1/2}e^{-(\eta_o-\eta)}\left[K_{1j}(\sin\eta + \cos\eta)\right.$$
$$\left. + K_{2j}(\cos\eta - \sin\eta)\right] \tag{66}$$

$$\frac{M_{\xi j}}{Eh^2} = \frac{1}{2}\left(\frac{r_o}{h}\right)^{-1/2}\left[3\left(1 - \nu^2\right)\right]^{-1/4}\lambda^{1/4}\left(1 + \lambda\xi^2\right)^{-1/8}\xi^{-1/2}e^{-(\eta_o-\eta)}\left[K_{1j}(\cos\eta - \sin\eta)\right.$$
$$\left. - K_{2j}(\sin\eta + \cos\eta)\right] - \frac{\alpha_s\,\Delta T}{12(1 - \nu)}\,\delta_{2j} \tag{67}$$

$$\frac{M_{\theta j}}{Eh^2} = \frac{\nu}{2}\left(\frac{r_o}{h}\right)^{-1/2}\left[3(1 - \nu)\right]^{-1/4}\lambda^{1/4}\left(1 + \lambda\xi^2\right)^{-1/8}\xi^{-1/2}e^{-(\eta_o-\eta)}\left[K_{1j}(\cos\eta - \sin\eta)\right.$$
$$\left. - K_{2j}(\sin\eta + \cos\eta)\right] - \frac{\alpha_s\,\Delta T}{12(1 - \nu)}\,\delta_{2j} \tag{68}$$

$$\frac{u_j}{h} = \bar{u}_j = \left(\frac{r_o}{h}\right)^{1/2}\left[3\left(1 - \nu^2\right)\right]^{1/4}\lambda^{1/4}\left(1 + \lambda\xi^2\right)^{-1/8}\xi^{1/2}e^{-(\eta_o-\eta)}\left[K_{1j}(\sin\eta + \cos\eta)\right.$$
$$\left. + K_{2j}(\cos\eta - \sin\eta)\right] + \frac{r_o}{h}\,\xi\alpha_s T_s\delta_{1j} \tag{69}$$

$$\frac{w_j}{h} = \bar{w}_j = -\left(\frac{r_o}{h}\right)^{1/2}\left[3\left(1 - \nu^2\right)\right]^{1/4}\lambda^{-1/4}\left(1 + \lambda\xi^2\right)^{1/8}\xi^{-1/2}e^{-(\eta_o-\eta)}\left[K_{1j}(\cos\eta + \sin\eta)\right.$$
$$\left. + K_{2j}(\cos\eta - \sin\eta)\right] + \frac{1}{2}\frac{r_o}{h}\lambda^{1/2}\xi^2\alpha_s T_s\delta_{1j} + \tilde{w}_j \tag{70}$$

$$\beta_j = 2\sqrt{3\left(1 - \nu^2\right)}\left(1 + \lambda\xi^2\right)^{1/8}\xi^{-1/2}e^{-(\eta_o-\eta)}\left(K_{1j}\cos\eta - K_{2j}\sin\eta\right) \tag{71}$$

where δ_{ij}, called Kronecker delta, is defined as

$$\left.\begin{aligned} \delta_{ij} &= 1 \qquad (i = j) \\ \delta_{ij} &= 0 \qquad (i \neq j) \end{aligned}\right\} \tag{72}$$

and constants $\tilde{w}_j$ representing nondimensional rigid body translations are to be determined from the boundary condition on w. The total value of a quantity is therefore the sum of the components (for example, $\beta = \beta_1 + \beta_2 + \beta_3$).

RESULTS AND DISCUSSION

Stresses and deformations throughout a paraboloid shell with a ring attached at the edge can be calculated from equations (64) to (71). Because the rotation of the tangent β has the most significant effect on solar concentrator performance, results are presented for the variation of β with radial distance for two types of temperature distributions and various values for the structural and geometric parameters. The temperature distributions represented are (1) uniform temperature change of the shell and a possibly different temperature change of the ring from the datum temperature (consideration of $\alpha_r T_r - \alpha_s T_s$), and (2) uniform temperature gradient through the thickness of the shell with its middle surface and the ring at the datum temperature (consideration of $\alpha_s \Delta T$). Finally, results are presented of simplified efficiency calculations described in the appendix to give some idea of the influence of these thermal loadings on the performance of a solar concentrator.

Effect of Temperature Difference Between Shell and Ring

The rotation of the tangent to the shell β as a function of radial distance r/r_o is shown in figures 4 to 9 for temperature distribution $\alpha_r T_r - \alpha_s T_s$. All results are for $\lambda = 1/3$ (except fig. 7), $r_o/h = 5000$ (except fig. 8), and no ring eccentricities (except fig. 9). In figures 4 to 9 for the case of the same material in the ring and the shell and the same uniform temperature change in the ring and the shell, no rotations occur anywhere. It must be borne in mind that the slope changes presented in this set of figures are those of a material point of the shell and are not necessarily those of a spatial coordinate. In temperature distribution $\alpha_r T_r - \alpha_s T_s$ the T_s component causes the shell to experience an expansion, and at a spatial coordinate there is a slope change because one material point is replaced by another material point which has a different slope than the original point. In this instance most of the paraboloid has expanded to the shape of a new paraboloid which has its focal length $1 + \alpha_s T_s$ times as large as the original focal length.

Results for various values of the relative extensional and flexural stiffness parameters $\overline{C}$ and $\overline{D}$ for a constant ratio of $\overline{D}$ to $\overline{C}$ $\left(\overline{D}/\overline{C} = 10\ 000\right)$ are shown in figure 4. For small values of $\overline{C}$ and $\overline{D}$ the ring stiffnesses are small relative to those of the shell, and the shell is relatively unaffected by the presence of the ring. As the values of $\overline{C}$ and $\overline{D}$ are increased, the region near the edge of the shell is beginning to be affected by the presence of the ring. When the values of $\overline{C}$ and $\overline{D}$ approach infinite values, the edge of the shell becomes "clamped." In this condition rotation of the tangent to the shell at the edge is not allowed, and the radial displacement is constrained to be the same as that of the ring caused by the temperature change of the ring.

Results for a large value of the relative flexural stiffness parameter, $\overline{D} = 10\ 000$, coupled with various values of $\overline{C}$, and results for a moderately large value of the relative extensional parameter, $\overline{C} = 0.1$, coupled with various values of $\overline{D}$ are shown in figures 5 and 6, respectively. Effects of variations in the shape parameter λ and variations in the radius-thickness ratio r_o/h are shown in figures 7 and 8, respectively, for infinitely large values of both $\overline{C}$ and $\overline{D}$. As the shell becomes flatter (λ decreasing or rim angle decreasing), the rotations become larger in magnitude everywhere in the edge region and the edge effects are propagated farther into the shell (fig. 7). Thus from the point of view of keeping shell rotations small, larger rim angles are desirable. Finally, the influence of small axial eccentricities of the ring are illustrated in figure 9. Effects of small radial eccentricities of the ring are not shown because they are negligible.

Effect of Temperature Gradient Through Thickness of Shell

The rotation of the tangent to the shell β as a function of radial distance r/r_o is shown in figures 10 to 12 for temperature distribution $\alpha_s \Delta T$. The effects of various values of the relative stiffness parameters $\overline{C}$ and $\overline{D}$ for a constant ratio of $\overline{D}/\overline{C} = 10\ 000$ are shown in figure 10 for a shell for which $\lambda = 1/3$ and $r_o/h = 5000$. As the values of both C and D approach infinitely large values, β approaches zero throughout the shell. The free edge case where $\overline{C} = \overline{D} = 0$, on the other hand, leads to the largest rotations. Effects of variation in the shape parameter λ are shown in figure 11 for $r_o/h = 5000$ for the free edge case. As in the case of temperature distribution $\alpha_r T_r - \alpha_s \Delta T$, larger values of λ lead to reduced magnitudes of rotation. The results of linear flat-plate theory used for preliminary studies such as reference 1 for which

$$\frac{\beta}{\alpha_s \Delta T} = \frac{r_o}{h}\frac{r}{r_o} \tag{73}$$

are not given in this figure since values obtained from this formula are found to be much larger and affect the entire shell. Finally, effects of variations in r_o/h are shown in figure 12 for $\lambda = 1/3$ for the free edge case.

Influence of Thermal Effects on Concentrator Performance

The loss in efficiency due to thermal distortions based on the assumptions and analysis contained in the appendix is shown in figures 13 and 14. It is emphasized that these results are based on the assumption that solar energy is coming from a point source. Furthermore, interaction of thermal distortions with other features which reduce efficiency has not been incorporated. The effect on efficiency of temperature distribution $\alpha_r T_r - \alpha_s T_s$ is shown in figure 13 when ΔT is zero, and the effect of temperature distribution $\alpha_s \Delta T$ when $\alpha_r T_r - \alpha_s T_s$ is zero is shown in figure 14.

The effect of temperature distribution $\alpha_r T_r - \alpha_s T_s$ on efficiency is shown in figure 13 for a shell having values of $\lambda = 1/3$, $r_o/h = 5000$, and $\nu = 0.3$. The shell has an attached ring with properties such that $\overline{C} = 1$ and $\overline{D} = 10^6$ which simulates one of the most detrimental conditions. The efficiency is shown as a function of the area concentration ratio, herein used as the ratio of the projected area of the paraboloid to the area of the aperture of an absorber in the focal plane, for values of $\left|\alpha_r T_r - \alpha_s T_s\right|$ equal to 100, 50, 20, and 10 μin./in. (μm/m). When $\alpha_r = \alpha_s = 10$ μin./in-^oF $\left(18 \frac{\mu m}{m\text{-}^oK}\right)$, which is roughly the value of this coefficient for metals, these curves correspond to 10^o F (5.6^o K), 5^o F (2.8^o K), 2^o F (1.1^o K), and 1^o F (0.56^o K).

The effect of temperature distribution $\alpha_s \Delta T$ on efficiency is shown in figure 14 for a shell having values of $r_o/h = 5000$, $\nu = 0.3$, and $\lambda = 1/3$. The shell does not have an attached ring and this case leads to the greatest losses in efficiency due to a temperature gradient through the thickness of the shell. Curves are presented for four values of $\alpha_s \Delta T$. Since the area in which thermal distortions occur is small, it is not surprising that the loss in efficiency is not great.

CONCLUDING REMARKS

Linear equations are presented to describe the action of a paraboloid under axisymmetric temperature loading consisting of a constant temperature change of the shell, constant temperature gradient through the thickness of the shell, and a constant temperature change of an attached ring. Slope distortions are found to be confined to a region near the edge of the shell and it is found that larger rim angles are desirable since they restrict the distortions to smaller magnitudes and to a smaller region.

For the case of a paraboloidal shell with a free edge subjected to a constant temperature gradient through its thickness, the results for preliminary purposes based on flat-plate formulas indicate the entire surface is affected and the rotations involved are much greater than those determined by the present analysis. It is found that an attached ring relieves the distortions due to a temperature gradient through the thickness of the shell. The attached ring however becomes the source of loading on the shell when the shell is at one temperature and the ring at another temperature. The larger the ratio of the extensional stiffness of the ring compared with that of the shell, the greater the distortions.

Langley Research Center,
National Aeronautics and Space Administration,
Langley Station, Hampton, Va., April 19, 1966.

APPENDIX

EFFICIENCY CONSIDERATIONS

The objective of this appendix is to estimate the loss in concentrating efficiency due to thermal distortions. The concentrating efficiency used herein is defined to be the ratio of the specularly reflected energy directed within a prescribed area in the focal plane divided by the total specularly reflected energy (shadowing effects of the absorber being neglected). A point source of energy is treated. From this simplified analysis an idea might be gained as to the influence of temperature differences on the performance of a solar concentrator. The interactions of thermal distortions with other features which also reduce the efficiency of the collecting system such as, the sun's finite image, irregularities in the concentrator surface, and so forth, have not been included.

Consider the reflecting surface being distorted at a point such that a ray which originally was directed to the focus is now displaced a distance l in the focal plane. The point under consideration is shown in figure 15 after the reflecting surface has undergone a positive rotation. Attention here is restricted to a point within the region near the edge of the shell for which consideration of the effect of the rotation alone is sufficient since it can be shown that the effects of vertical and radial displacements are of higher order.

When transverse shearing deformations are neglected as was done in the shell development, the rotation of the tangent to the reflecting surface is the same as the rotation of the tangent to the middle surface β which can be determined from equation (71). From the geometry of figure 15,

$$l = r - (f - z)\tan(2\varphi - 2\beta) \tag{A1}$$

Nondimensionalization of equation (A1) by dividing by r_o yields

$$\frac{l}{r_o} = \beta \frac{4\xi}{\sin 4\varphi} \tag{A2}$$

where geometrical considerations have been employed and in the expansion of $\tan(2\varphi - 2\beta)$ in powers of β, β^2 and higher terms have been neglected. Equation (A2) may be rewritten as

$$\frac{l}{r_o} = \lambda^{-1/2} \frac{\left(1 + \lambda\xi^2\right)^2}{1 - \lambda\xi^2} \beta \tag{A3}$$

where $\sin 4\varphi$ has been expressed as a function of ξ, after φ has been determined through the use of equations (35), (36), and equation (13b) to be

$$\varphi = \tan^{-1}\left(\lambda^{1/2}\xi\right) \tag{A4}$$

If an absorber has a flat circular aperture of radius l_a in the focal plane,

$$\frac{l_a}{r_o} = \frac{1}{\sqrt{C_A}} \tag{A5}$$

where C_A is the area concentration ratio herein defined as the ratio of the projected area of the paraboloid to the area of the aperture of the absorber. At a particular point, r/r_o, if the absolute value of l/r_o determined from equation (A3) is greater than $1/\sqrt{C_A}$, the reflected energy from that point is considered lost and if the absolute value of l/r_o is less than $1/\sqrt{C_A}$, the reflected energy from that point is considered to be collected. For a particular value of the concentration ratio, the projected area of the concentrator from which energy is collected can be found graphically and the ratio of this area to the total concentrator projected area is the efficiency. The results shown in figures 13 and 14 are obtained by selecting several values of the concentration ratio and calculating the corresponding efficiency.

REFERENCES

1. Dresser, D. L.: Elements of Solar Collector Design. Paper No. 61-24, Inst. Aerospace Sci., Jan. 1961.

2. Stern, G. S.: Thermoelastic Analysis of a Parabolic Shell. Tech. Rept. No. 32-479, Jet Propulsion Lab., Calif. Inst. Technol., Aug. 1, 1963.

3. Mechtly, E. A.: The International System of Units – Physical Constants and Conversion Factors. NASA SP-7012, 1964.

4. Reissner, Eric: On the Theory of Thin Elastic Shells. Reissner Anniversary Volume: Contributions to Applied Mechanics, J. W. Edwards, 1949, pp. 231-247.

5. Hildebrand, F. B.: On Asymptotic Integration in Shell Theory. Elasticity, McGraw-Hill Book Co., Inc., 1950, pp. 53-66.

6. Lur'e, A. I.: Statics of Thin-Walled Elastic Shells. AEC-tr-3798, U.S. At. Energy Comm., Oct. 1959.

7. Novozhilov, V. V. (P. G. Lowe, trans.): The Theory of Thin Shells. P. Noordhoff, Ltd. (Groningen, The Netherlands), c.1959.

8. Flügge, Wilhelm: Stresses in Shells. Second printing, Springer-Verlag (Berlin), 1962.

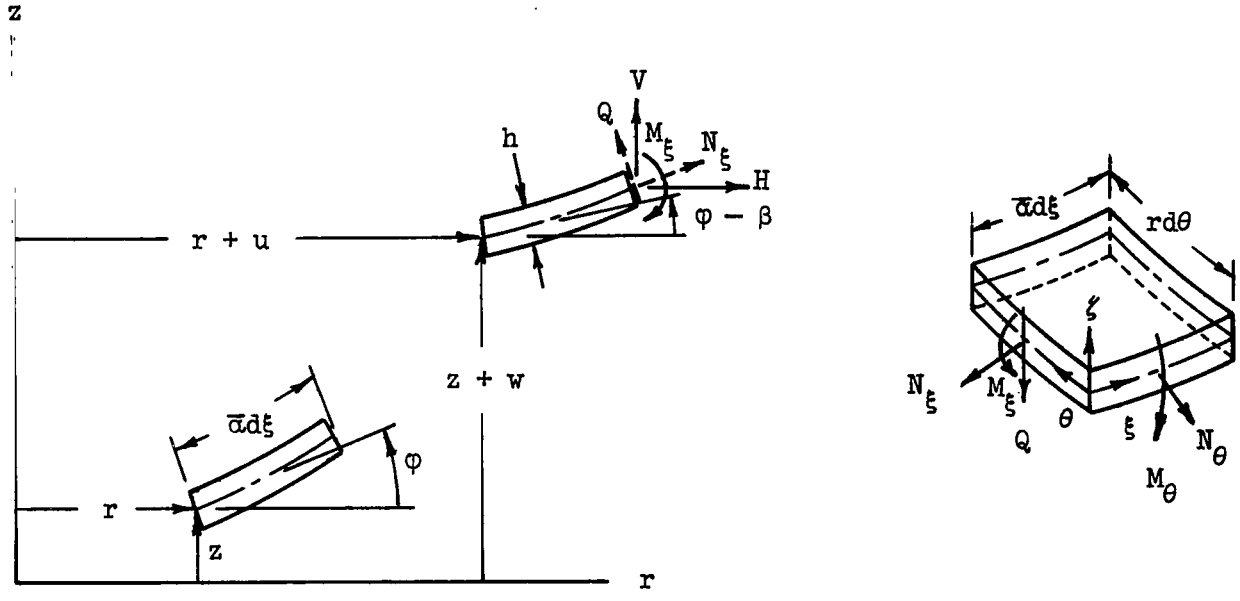

(a) Side view of shell element in undeformed and deformed positions.

(b) Shell element.

Figure 1.- Stress resultants, couples, and displacements.

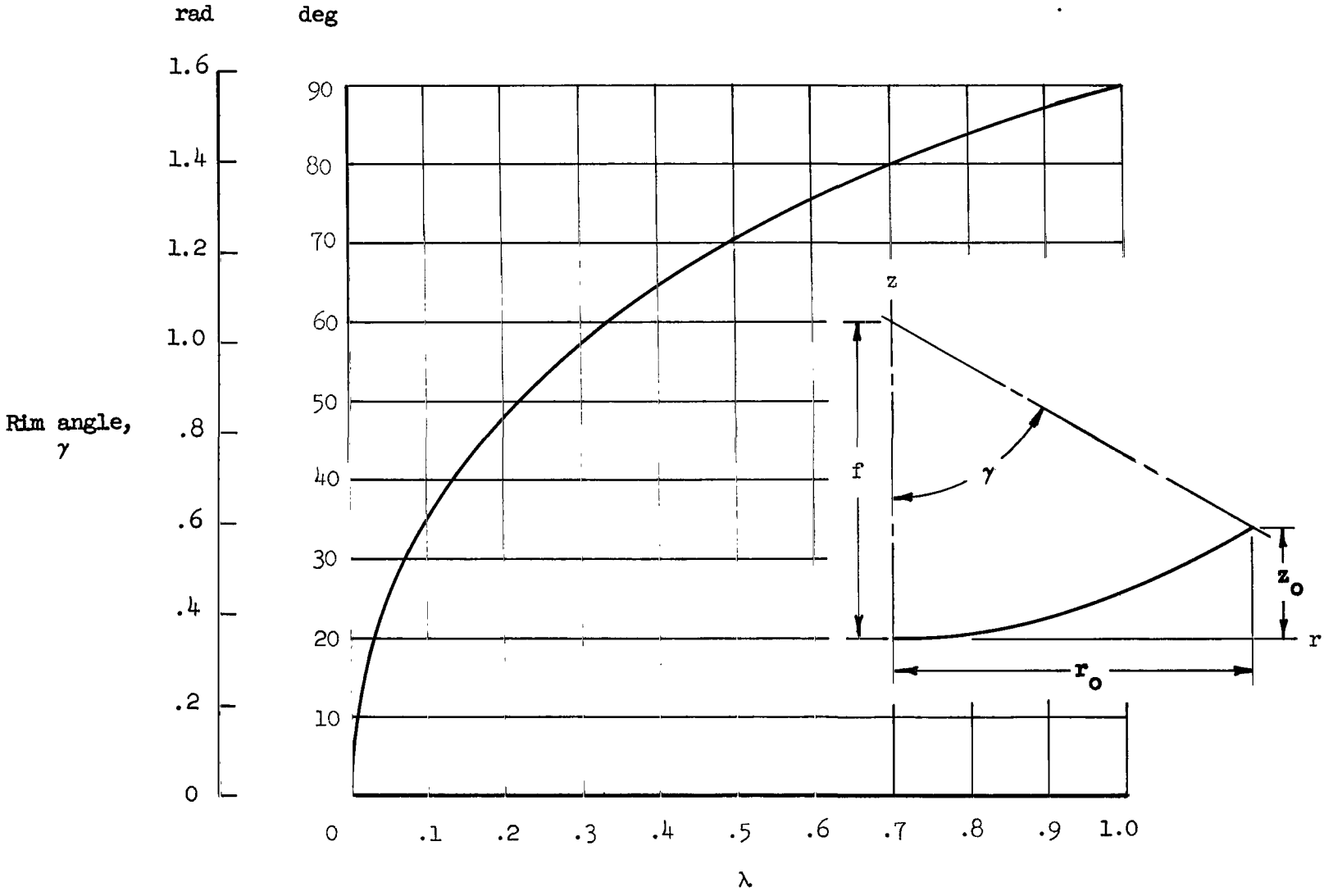

Figure 2.- Relationship of rim angle to parameter indicating amount of concavity of paraboloid. $\lambda = (r_o/2f)^2$.

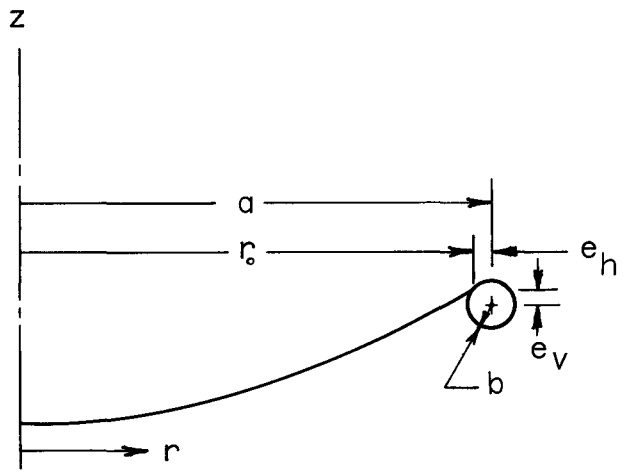

(a) Geometry of shell-ring structure.

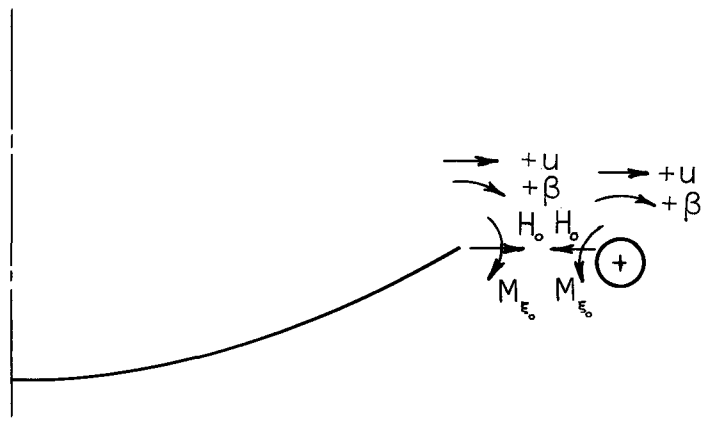

(b) Internal reactions at attachment point of ring to shell.

Figure 3.- Geometry and internal reactions on an axial section of shell-ring structure.

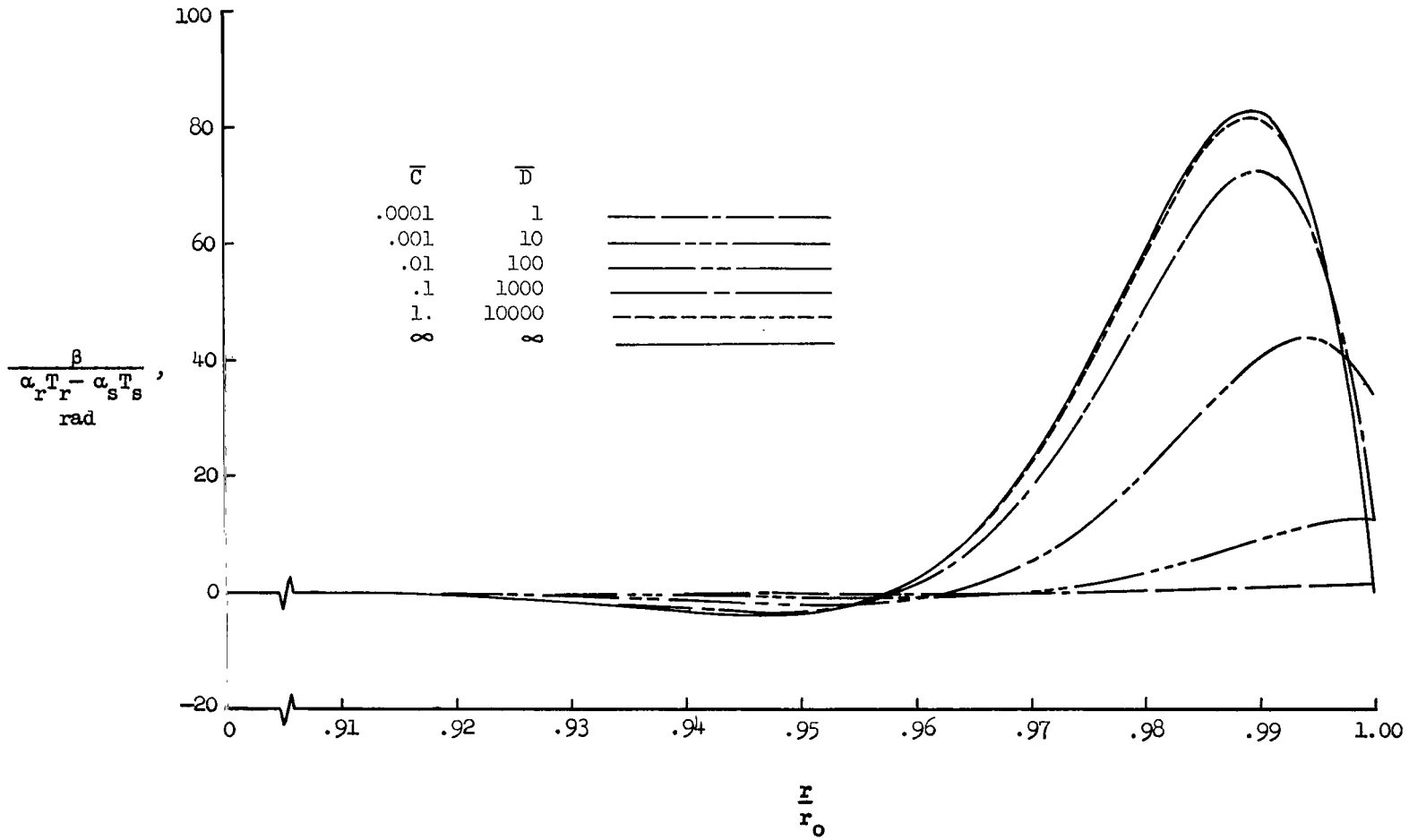

Figure 4.- Effect of relative extensional and bending stiffness of a ring on rotation of tangent to shell near edge due to a temperature difference between ring and shell. $\Delta T = 0$; constant T_r; constant T_s; $\nu = 0.3$; $\lambda = 1/3$; $r_o/h = 5000$; $e_v = 0$; $e_h = 0$.

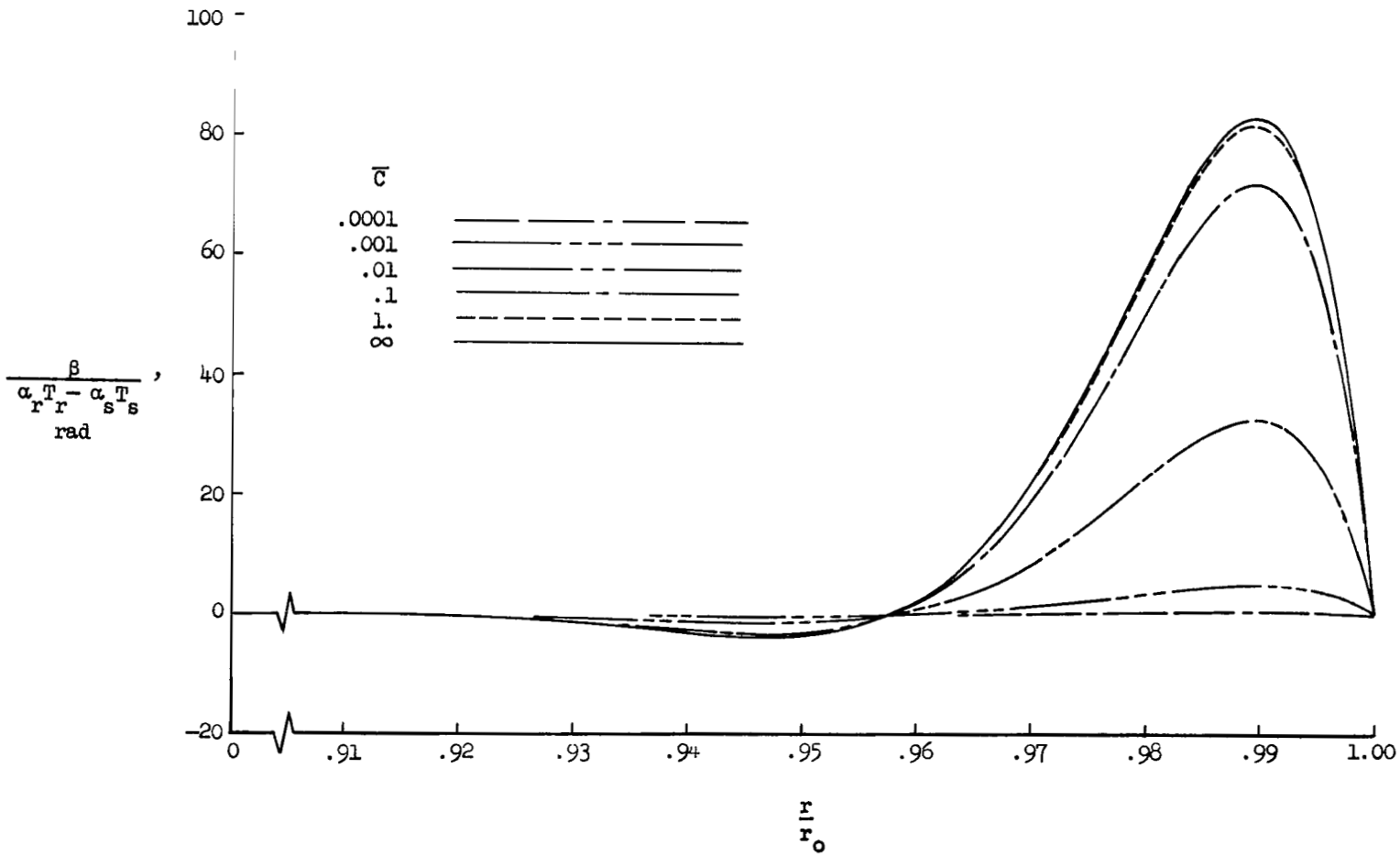

Figure 5.- Effect of relative extensional stiffness of a ring of constant bending stiffness on rotation of tangent to shell near edge due to a temperature difference between ring and shell. $\Delta T = 0$; constant T_r; constant T_s; $\nu = 0.3$; $\lambda = 1/3$; $r_o/h = 5000$; $\bar{D} = 10\,000$; $e_v = 0$; $e_h = 0$.

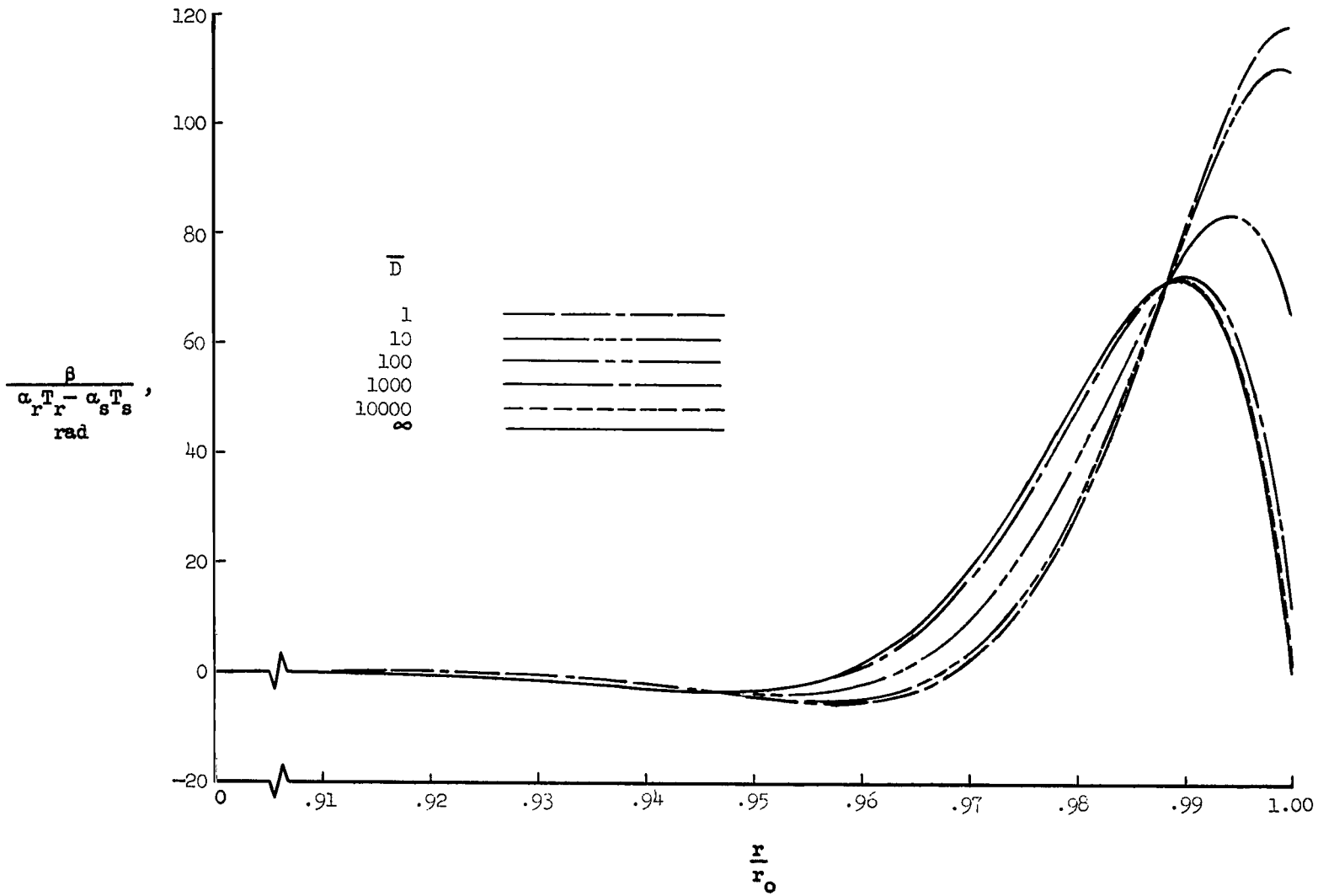

Figure 6.- Effect of relative bending stiffness of a ring of constant extensional stiffness on rotation of tangent to shell near edge due to a temperature difference between ring and shell. $\Delta T = 0$; constant T_r; constant T_s; $\nu = 0.3$; $\lambda = 1/3$; $r_o/h = 5000$; $\bar{C} = 0.1$; $e_v = 0$; $e_h = 0$.

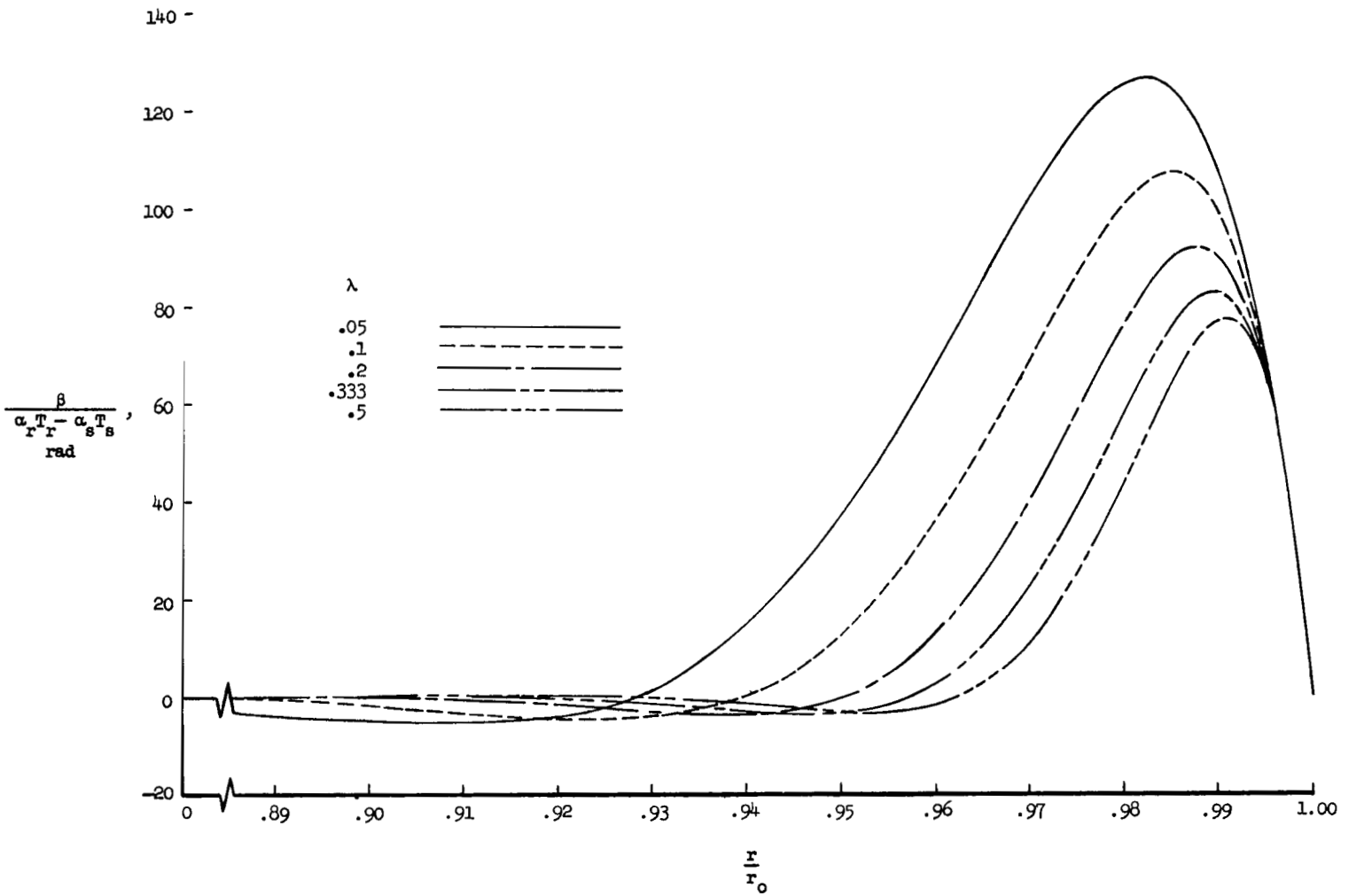

Figure 7.- Effect of shape parameter on rotation of tangent to shell near edge due to a temperature difference between ring and shell. $\Delta T = 0$; constant T_r; constant T_s; $\nu = 0.3$; $r_o/h = 5000$; $\bar{C} = \infty$; $\bar{D} = \infty$.

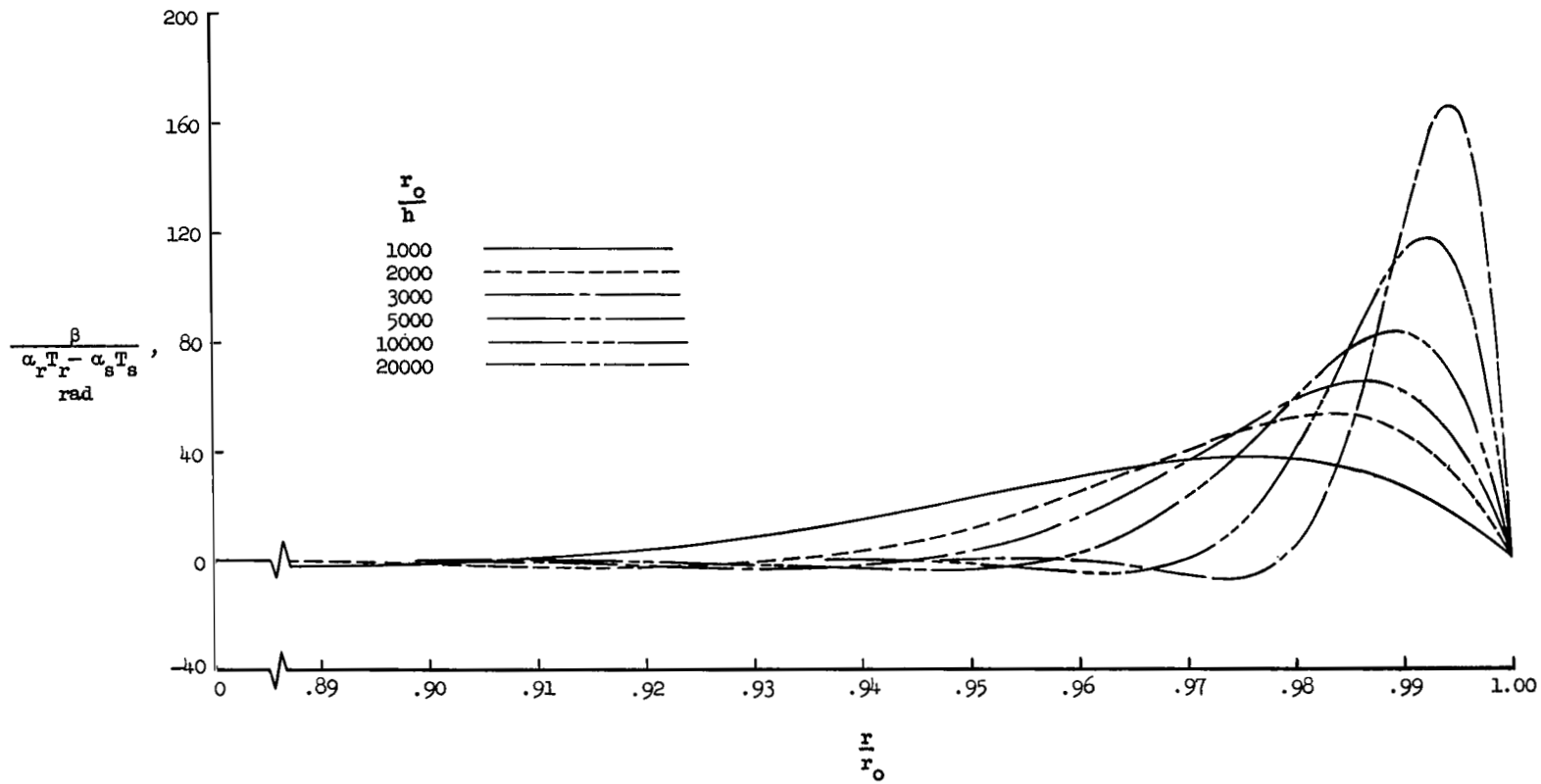

Figure 8.- Effect of r_0/h on rotation of tangent to shell near edge due to a temperature difference between ring and shell. $\Delta T = 0$; constant T_r; constant T_s; $\nu = 0.3$; $\lambda = 1/3$; $\bar{C} = \infty$; $\bar{D} = \infty$.

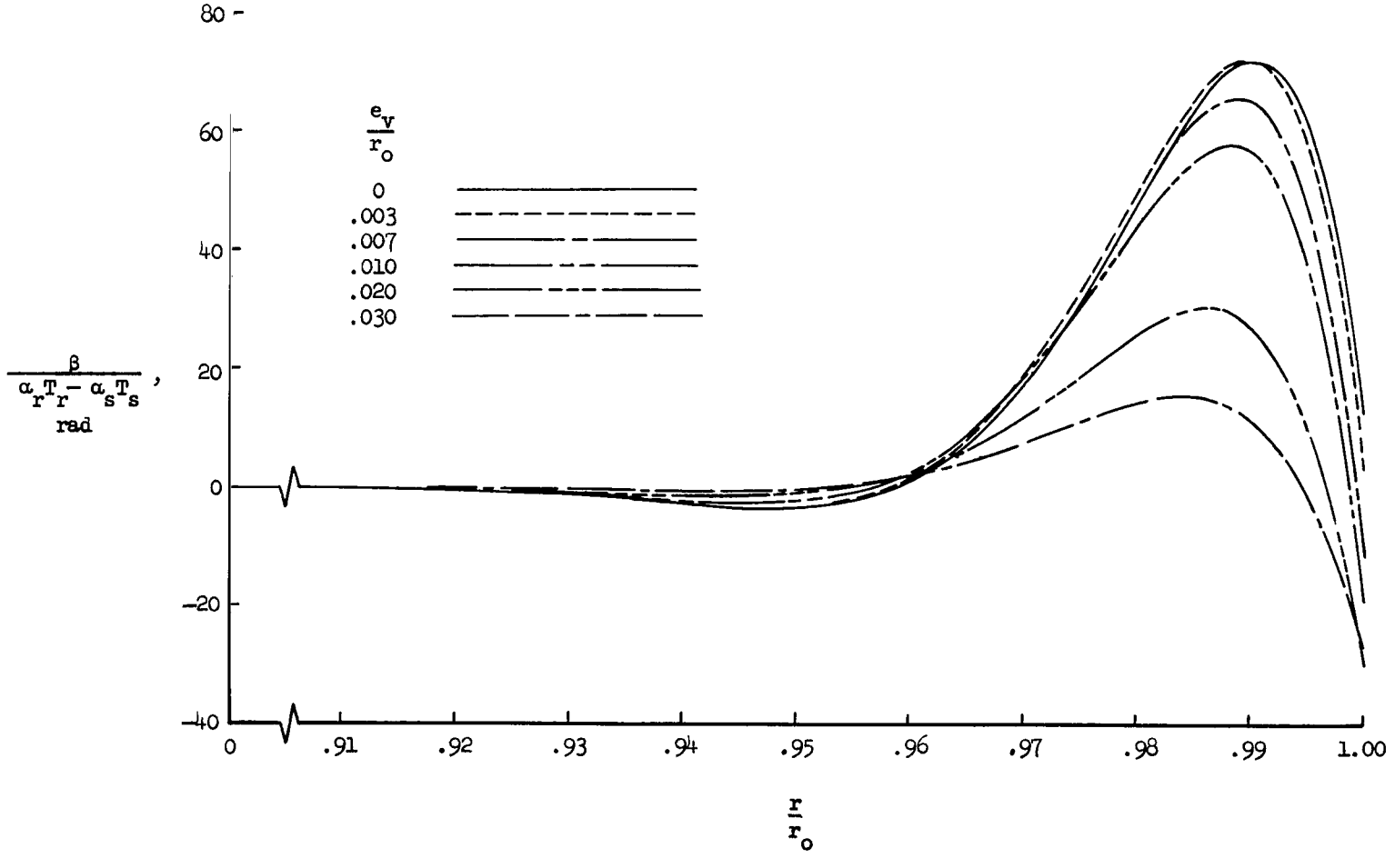

Figure 9.- Effect of axial eccentricity of ring on rotation of tangent to shell near edge due to a temperature difference between ring and shell. $\Delta T = 0$; constant T_r; constant T_s; $\nu = 0.3$; $\lambda = 1/3$; $r_o/h = 5000$; $\bar{C} = 0.1$; $\bar{D} = 10\,000$; $e_h = 0$.

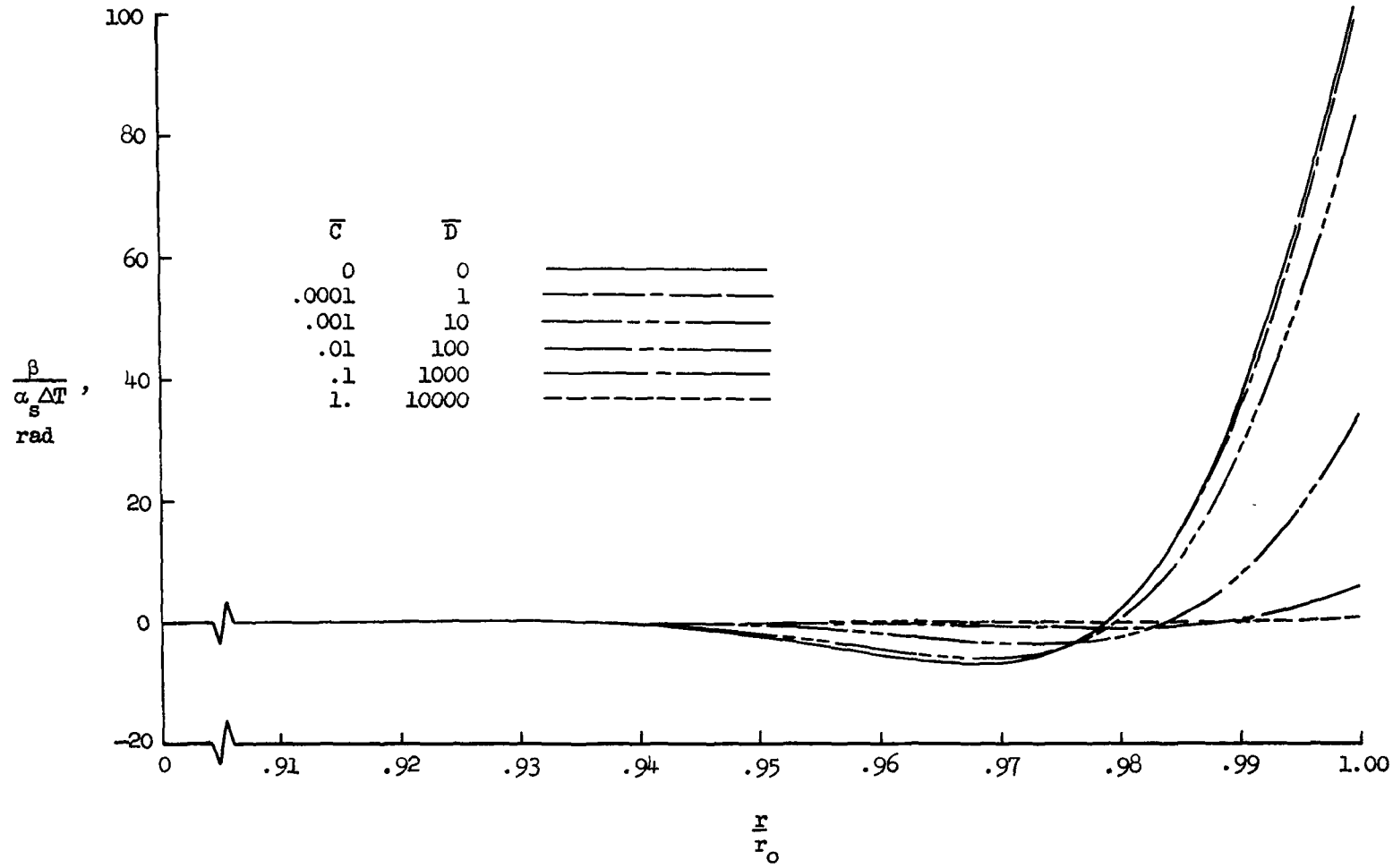

Figure 10.- Effect of relative extensional and bending stiffnesses of a ring on rotation of tangent to shell near edge due to a temperature gradient through thickness of shell. Constant ΔT; $\alpha_r T_r - \alpha_s T_s = 0$; $\nu = 0.3$; $\lambda = 1/3$; $r_o/h = 5000$; $e_v = 0$; $e_h = 0$.

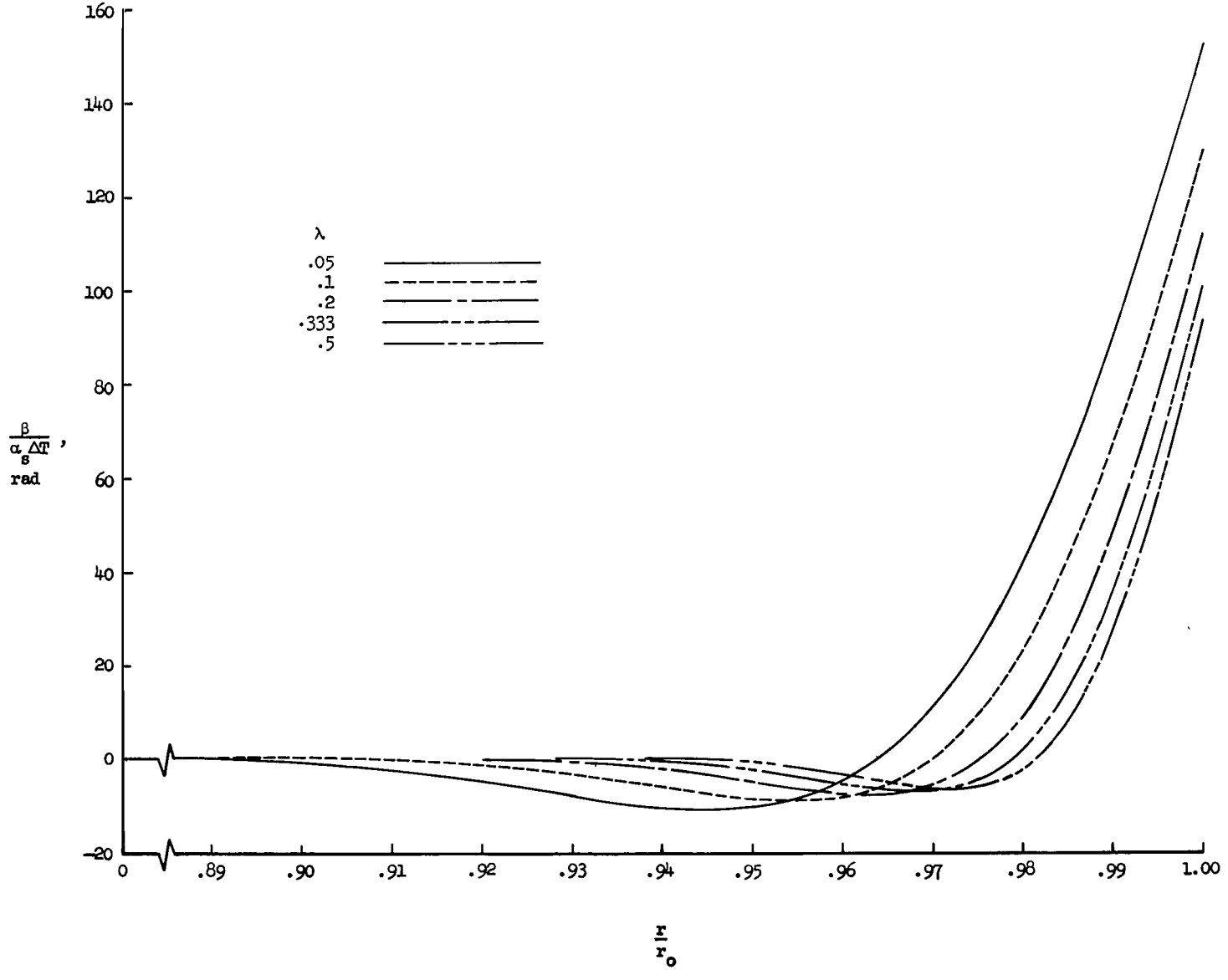

Figure 11.- Effect of shape parameter on rotation of tangent to shell near edge due to a temperature gradient through thickness of shell. Constant ΔT; $\alpha_r T_r - \alpha_s T_s = 0$; $\nu = 0.3$; $r_o/h = 5000$; $\bar{C} = 0$; $\bar{D} = 0$.

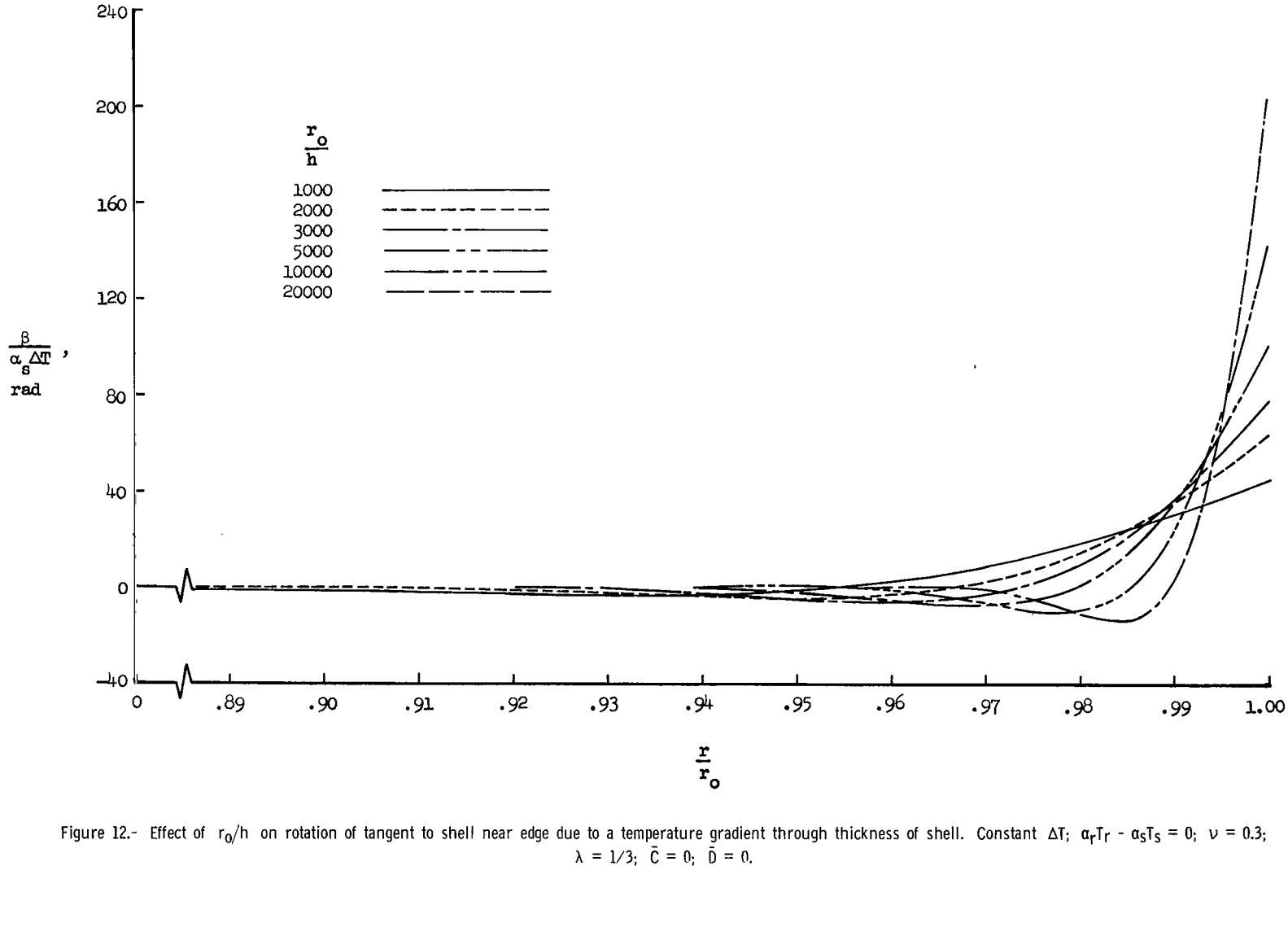

Figure 12.- Effect of r_o/h on rotation of tangent to shell near edge due to a temperature gradient through thickness of shell. Constant ΔT; $\alpha_r T_r - \alpha_s T_s = 0$; $\nu = 0.3$; $\lambda = 1/3$; $\bar{C} = 0$; $\bar{D} = 0$.

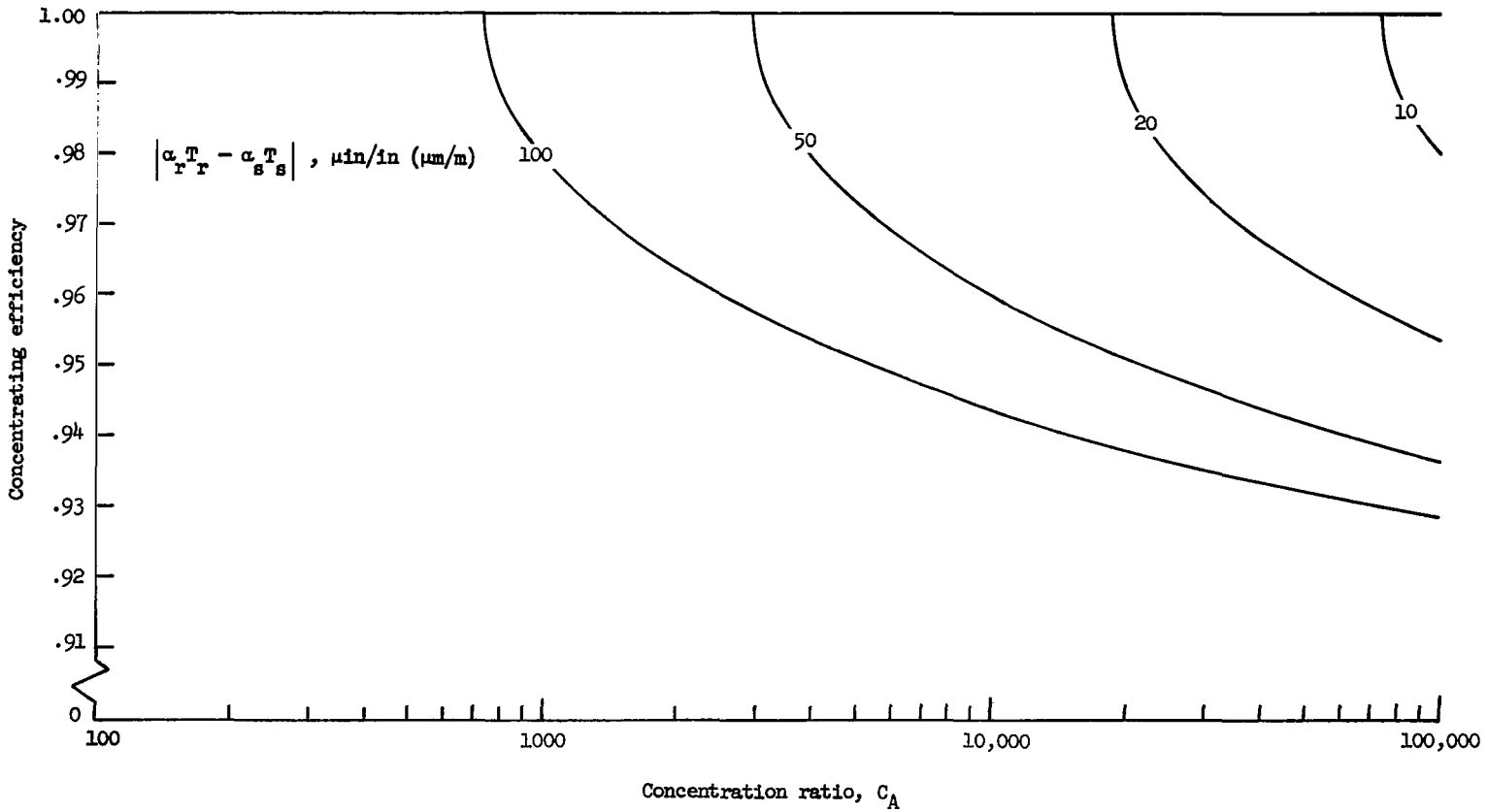

Figure 13.- Effect of thermal distortions near edge of a paraboloid due to a temperature difference between ring and shell on concentrating efficiency as a function of concentration ratio. Source of energy is treated as a point source. $\Delta T = 0$; constant T_r; constant T_s; $\nu = 0.3$; $\lambda = 1/3$; $r_o/h = 5000$; $\bar{C} = 1$; $\bar{D} = 10^6$; $e_v = 0$; $e_h = 0$.

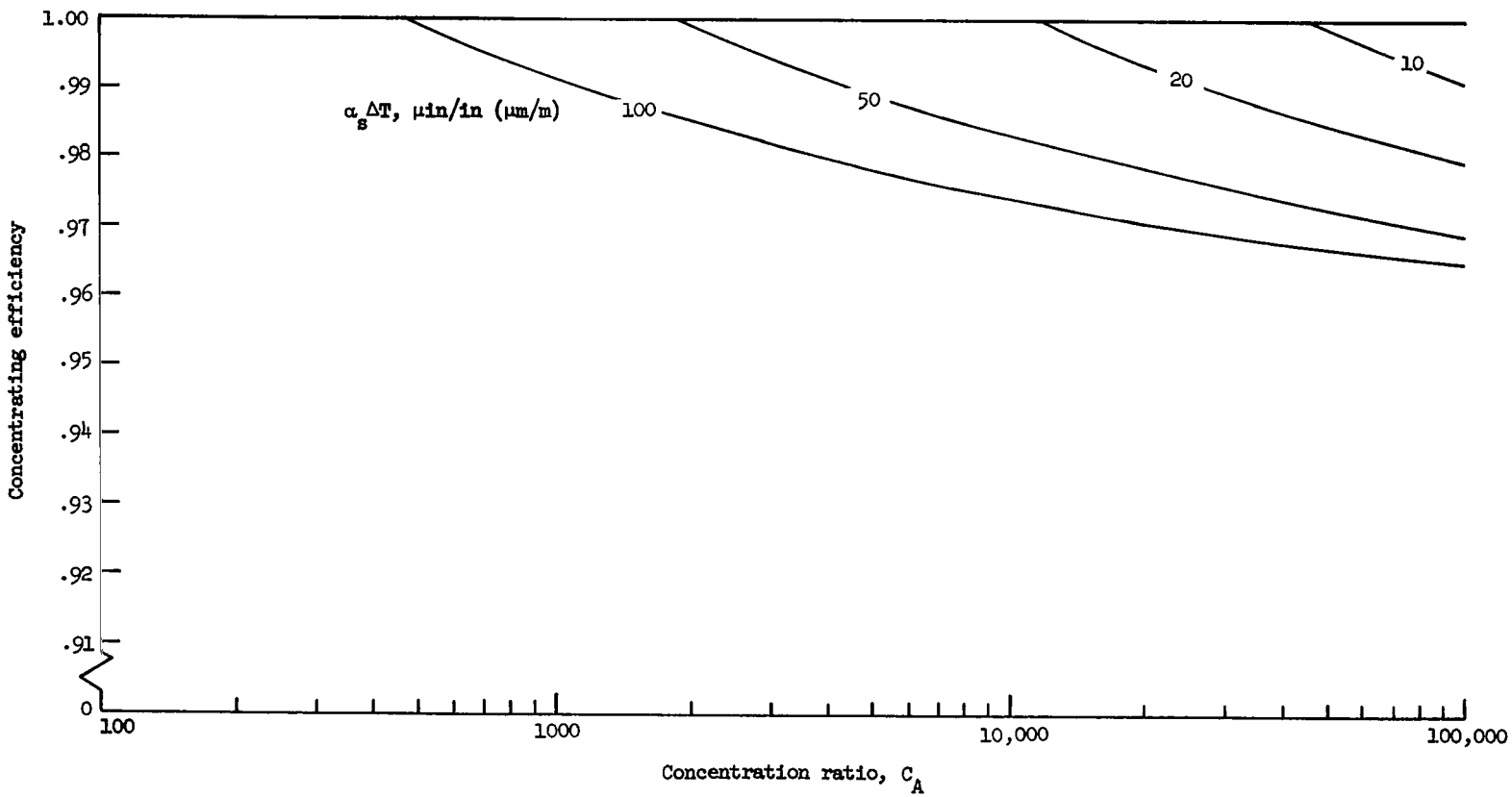

Figure 14.- Effect of thermal distortions near edge of a paraboloid due to a temperature gradient through thickness of shell on the concentrating efficiency as a function of concentration ratio. Source of energy is treated as a point source. Constant ΔT; $\alpha_r T_r - \alpha_s T_s = 0$; $\nu = 0.3$; $\lambda = 1/3$; $r_o/h = 5000$; $\bar{C} = 0$; $\bar{D} = 0$.

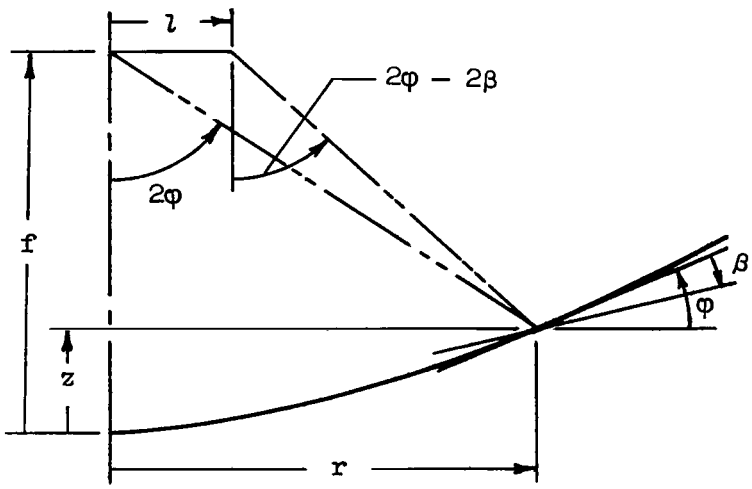

Figure 15.- Effect of rotation of tangent to shell on path of a reflected ray.

"The aeronautical and space activities of the United States shall be conducted so as to contribute . . . to the expansion of human knowledge of phenomena in the atmosphere and space. The Administration shall provide for the widest practicable and appropriate dissemination of information concerning its activities and the results thereof."

—NATIONAL AERONAUTICS AND SPACE ACT OF 1958

NASA SCIENTIFIC AND TECHNICAL PUBLICATIONS

TECHNICAL REPORTS: Scientific and technical information considered important, complete, and a lasting contribution to existing knowledge.

TECHNICAL NOTES: Information less broad in scope but nevertheless of importance as a contribution to existing knowledge.

TECHNICAL MEMORANDUMS: Information receiving limited distribution because of preliminary data, security classification, or other reasons.

CONTRACTOR REPORTS: Technical information generated in connection with a NASA contract or grant and released under NASA auspices.

TECHNICAL TRANSLATIONS: Information published in a foreign language considered to merit NASA distribution in English.

TECHNICAL REPRINTS: Information derived from NASA activities and initially published in the form of journal articles.

SPECIAL PUBLICATIONS: Information derived from or of value to NASA activities but not necessarily reporting the results of individual NASA-programmed scientific efforts. Publications include conference proceedings, monographs, data compilations, handbooks, sourcebooks, and special bibliographies.

Details on the availability of these publications may be obtained from:

SCIENTIFIC AND TECHNICAL INFORMATION DIVISION

NATIONAL AERONAUTICS AND SPACE ADMINISTRATION

Washington, D.C. 20546